PROCEEDINGS OF SPIE

On-chip Brillouin lasers based on 10 million-Q chalcogenide resonators without direct etch process

Sangyoon Han, Dae-Gon Kim, Joonhyuk Hwang, In Hwan Do, Dongin Jeong, et al.

SPIE.

Event: SPIE LASE, 2020, San Francisco, California, United States

On-chip Brillouin lasers based on 10 million-Q chalcogenide resonators without direct etch process

Sangyoon Han[a], Dae-Gon Kim[b], Joonhyuk Hwang[a], In Hwan Do[b], Dongin Jeong[b], Yong-Hee Lee[b], Duk-Yong Choi[*c], and Hansuek Lee[**a,b]

[a]Department of Physics, Korea Advanced Institute of Science and Technology, Daejeon 34141, Republic of Korea; [b]Graduate School of Nanoscience and Technology, Korea Advanced Institute of Science and Technology, Daejeon 34141, Republic of Korea; [c]Laser Physics Centre, Research School of Physics and Engineering, The Australian National University, Canberra, ACT 2601, Australia

ABSTRACT

We present a new device platform which defines on-chip chalcogenide waveguide/resonators without directly etching chalcogenide. Using our platform, we have demonstrated chalcogenide ring resonators with record high Q-factor exceeding 1.1×10^7 which is 10 times larger than previous record on on-chip chalcogenide resonators. A ring cavity is designed and fabricated for Stimulated Brillouin lasing on our platform. Thanks to the high-Q factor, Brillouin lasing with threshold power of 1 mW is demonstrated. This value is more than an order of magnitude improvement than previous world record for on-chip chalcogenide Brillouin lasers. We also developed an efficient and flexible method for resonator-waveguide coupling with our device platform. Coupling between a resonator and a waveguide can be varied from under-coupled region to over-coupled region.

Keywords: chalcogenide, resonator, Brillouin laser, high-Q, on-chip, low-threshold

1. INTRODUCTION

Large efforts have been made to implement on-chip optical devices using chalcogenide materials to make use of its high optical nonlinearities and its transparency to mid-infrared wavelength ranges up to 20 μm [1–8]. Despite the material's high optical non-linearities, the threshold powers of the chalcogenides-based non-linear devices are significantly high due to the low optical quality factors (on the order of 10^5) or high propagation loss (~ 1 dB/cm) of the chalcogenide devices. The low quality-factors of the devices are due to the high side wall roughness of the devices occurred during etching process for the chalcogenide films.

Here, we present a new device platform for on-chip chalcogenide devices which avoids direct etching of chalcogenide film. The geometries of the devices are defined not by etching of chalcogenide film but by pre-patterned silica substrate [9]. In this way, device fabrication is simply done by depositing chalcogenide on the pre-patterned substrate, and thus need for etching of chalcogenide is completely eliminated. As a result, the surface roughness of the chalcogenide devices is dramatically reduced. Using our new platform, we have made ring resonators and waveguides, and the quality factor of the resonators is measured as 11 million. This value of quality factor is 10 times larger than the previous record on on-chip chalcogenide devices fabricated using normal etching methods [3]. We have also demonstrated stimulated Brillouin lasing with the developed resonators. Thanks to the high-Q factor, the threshold power of the laser is below 1 mW which is more than 10 times smaller than the previous world record value of on-chip chalcogenide Brillouin lasers from other groups [4]. Cascaded lasing has been observed as well. Also, a flip-chip coupling scheme has been introduced to efficiently couple the resonators with on-chip waveguides. We believe that our new fabrication method shows a promising route to implement efficient non-linear chalcogenide devices on chips.

2. DESIGN OF TRAPEZOIDAL WAVEGUIDE STRUCTURE

The design of the waveguide cross-section based on the new fabrication process is shown in Fig. 1(a). A layer of chalcogenide (As_2S_3) film is deposited on top of the trapezoidal shaped SiO_2 layer. The thickness of the top region (= d)

E-mails of corresponding authors: *duk.choi@anu.edu.au, **hansuek@kaist.ac.kr

is thicker than the thickness of the side wings ($= d\cos\theta$), and therefore the top region has relatively higher index than the side wing regions. As a result, the optical mode is confined at the top of the trapezoid. This guiding principle of the trapezoidal waveguide is similar to rip-type waveguides [10] which is typically used for on-chip devices (Fig. 1(c)). As similar to the rib-type waveguides, the trapezoidal waveguide has three design parameters; film thickness (d), top width (w), and wedge angle (θ) of the trapezoid. By changing these parameters, the optical characteristics of the waveguide such as effective index, confinement and dispersion can be tuned. Figure 1(c) shows the simulated optical mode profile of fundamental mode of the trapezoidal waveguide at 1550 nm wavelength. For the simulation, w, d, and θ are set to 5 μm, 1.3 μm, and 30° respectively. The refractive index of the As_2S_3 film and the SiO_2 layer are set to 2.43 and 1.44, respectively. As shown in the figure, the optical mode is well guided at the center of the chalcogenide film.
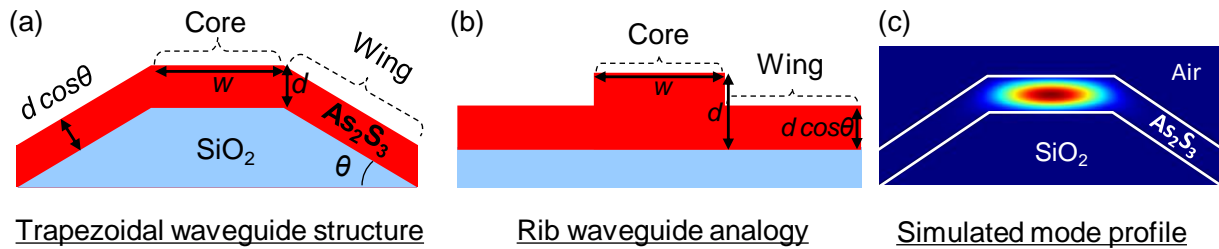

Figure 1. Structural descriptions of the trapezoidal waveguide. (a) Physical geometry of the trapezoidal waveguide. Chalcogenide film (As_2S_3) is deposited on top of the trapezoidal shape of the SiO_2 platform structure. The thickness of the core is d while the thickness of the wing is $d\cos\theta$ ($< d$). In this way, the effective index of the core is higher than the wing, and therefore optical mode is guided at the core by the index contrast. (b) The trapezoidal waveguide can be analogously understood by rib-type waveguide which is commonly used for on-chip waveguides. (c) Simulated mode profile of the fundamental mode of the trapezoidal waveguide. As shown in the figure, the optical mode is well confined at the core region.
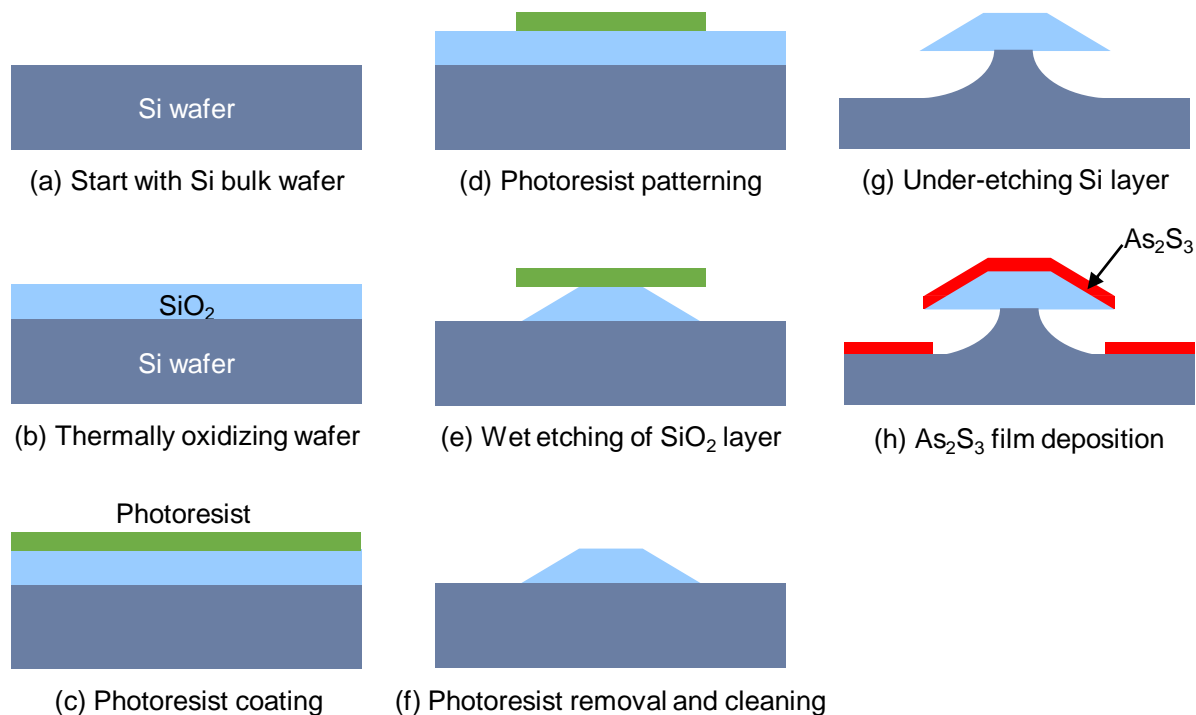
3. DEVICE FABRICATION

Figure 2. Detailed fabrication flow of the trapezoidal waveguide. (a) Fabrication is started with a silicon bulk wafer. (b) Thermal oxidation process is done on the wafer to grow 8 μm-thick SiO_2 layer on the surface of the wafer. (c) Standard I-line photoresist is

coated on the surface of the wafer by spin coating. Adhesion promoter is applied on the surface of the wafer before coating to control the adhesion between the photoresist and the wafer. (d) Photoresist is patterned with standard photolithography method (exposure and develop) to be used for wet-etching mask. (e) Hydrofluoric acid is used to wet-etch SiO_2 layer. The etching angle is determined by the adhesion property of the photoresist controlled at the photoresist coating step. (f) The photoresist is removed and the wafer is thoroughly cleaned with acetone, IPA, and water. (g) XeF_2 gas is used to isotropically under-etch the silicon substrate under the SiO_2 platform. Etch depth is ~ 15 µm. (h) As_2S_3 film is deposited on top of the SiO_2 platform structure with thermal evaporation process under high vacuum for directional deposition. 2 nm-thick Al_2O_3 layer is coated around the structure to passivate the As_2S_3 film by atomic layer deposition (ALD) method.

The details for fabricating the trapezoidal waveguide is shown in Fig. 2. The fabrication process starts with a bulk silicon wafer (Fig. 2(a)). Using thermal oxidation method, 8 µm-thick grown SiO_2 film is grown on the surface of the wafer (Fig. 2(b)). Standard I-line photoresist is spin coated on the SiO_2 film (Fig. 2(c)). Adhesion promotor is applied on the surface to control adhesion of the photoresist prior to photoresist coating. The angle (θ) of the trapezoid is controlled by the adhesion property as similar to reference 9. The coated photoresist is exposed with photomask using mask-aligner. Photoresist development process is then followed to pattern the photoresist as a wet-etching mask (Fig. 2(d)). The wet-etching of SiO_2 layer is done by hydrofluoric acid (HF) solution to make the trapezoidal pattern (Fig. 2(e)). After wet-etching step, the photoresist is removed with acetone and IPA, and the wafer is cleaned thoroughly (Fig. 2(f)). Then isotropic dry etching with XeF_2 gas is introduced to under etch silicon under the SiO2 trapezoidal platform (Fig. 2(g)). The under etching of the silicon is to prevent leakage of the optical mode to the silicon substrate from the trapezoidal waveguide. A thermal evaporation step is followed under a high-vacuum to directionally deposit 1.3 µm-thick As_2S_3 film on the wafer (Fig. 2(h)). As a final step, 2 nm-thick Al_2O_3 layer is conformally deposited on the wafer for surface passivation with atomic layer deposition (ALD) method. By having the thin Al_2O_3 layer, the chalcogenide film is protected by potential contaminations such as surface oxidation and water absorption.
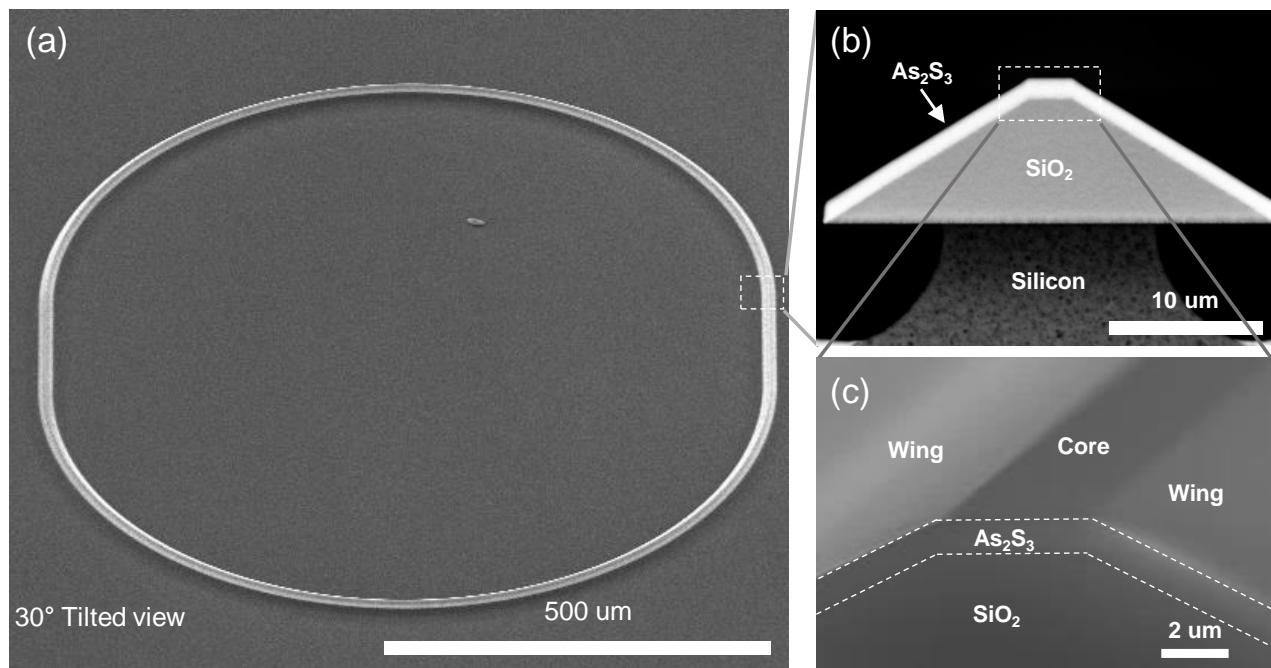

Figure 3. Scanning electron microscope (SEM) image of the fabricated device. (a) Overview image of racetrack resonator fabricated with the new proposed fabrication method. The image is taken with 30º tilted view. (b) Cross-sectional SEM image of the trapezoidal waveguide structure. (c) Zoom-in view of cross-section of the trapezoidal waveguide. As shown in the image, the surface of the core and the wing of the waveguide is very smooth (roughness is below 1 nm confirmed by AFM measurement).

Figure 3(a) shows the scanning electron microscopy (SEM) image of the racetrack resonator having the trapezoidal cross-section fabricated with the proposed fabrication process (The image is taken with 30º tilted view). Figure 3(b) shows the SEM image of cross-section of the trapezoidal waveguide, and Fig. 3(c) shows the zoom-in view of the cross-section and the top surface of the waveguide. As shown in the image, the surface of the waveguide is very smooth. The roughness of the top surface of the waveguide is measured using atomic force microscopy (AFM), and the surface roughness is measured

below 1 nm (root mean square value). It confirms that the proposed fabrication method indeed reduces the surface roughness of the chalcogenide device dramatically.

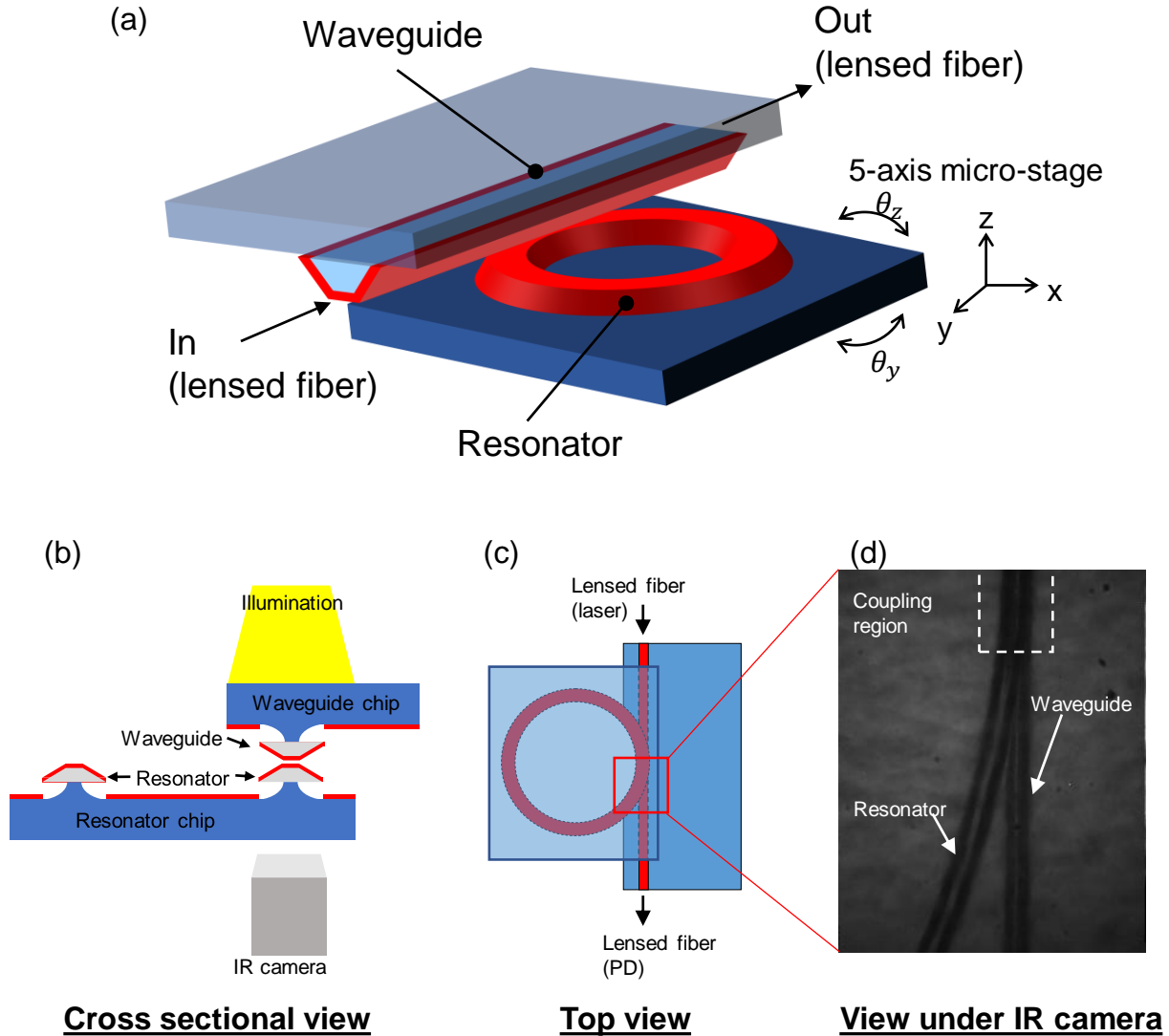## 4. FLIP-CHIP COUPLING SCHEME FOR EFFICIENT RESONATOR-WAVEGUIDE COUPLING

Figure 4. Description of the flip-chip coupling method to couple the resonator with an on-chip waveguide. (a) Overview of the flip-chip coupling method. The waveguide chip is flip on top of the resonator chip to bring the waveguide and the resonator in proximity distance. The resonator chip is mounted on a 5-axis micro-stage to allow fine alignment. Lensed fibers are end-fire coupled to the waveguide facet to insert and collect light from the waveguide. (b) Cross-sectional view of the flip-chip coupling scheme. Infrared imaging setup is used to view the resonator and the waveguide through the silicon substrate. Halogen lamp illuminates the structures from the opposite side of the microscope objective. (c) Top view of the coupling scheme. (d) Infrared image of the aligned resonator and the waveguide taken using the imaging setup.

For efficient operation of resonator-based devices, it is important to have effective coupling method to couple light in and out of the resonator. To have high coupling efficiency, phase matching between the resonator and a waveguide is required [11]. Silica tapered fibers are widely used option for efficient resonator-waveguide coupling [12–14]. However, it cannot be used

for chalcogenide resonators due to high index of chalcogenide film. To efficiently couple light into the chalcogenide resonators, we developed a flip-chip coupling scheme (Fig. 4(a)). A waveguide having same cross-sectional geometry as the resonator is fabricated with the same fabrication method for coupling. Since the effective index of the waveguide is fully determined by its cross-sectional geometry, the resonator and the waveguide have same refractive index. Therefore, they are perfectly phase matched and exhibit good coupling characteristics. The waveguide chip is flipped on top of the resonator chip for evanescent coupling between the resonator and the waveguide. The resonator chip in mounted on a five-axis micro-stage (x,y,z, θ_y, and θ_z) to accurately align the relative position between the top of the resonator and the top of the waveguide for efficient coupling. The relative tilt (θ_y, θ_z) between the two chips are adjusted to bring to chip in parallel. When the two chips are brought in proximity distance, an infrared imaging setup is used to see the resonator and the waveguide for fine alignment (Fig. 4(b)). For illumination, halogen lamp is illuminated towards the objective lens. Since silicon is transparent to infrared wavelength, the infrared camera can the relative distance between the resonator and the waveguide (Fig. 4(c), (d)). Using the flip-chip coupling method, we have confirmed that the coupling efficiency can be achieved more than 90 %. To couple the waveguide with a tunable laser and a photodetector, we couple the waveguide with end-firing method using two lensed fibers at each end.

5. QUALITY FACTOR MEASUREMENT AND BRILLOUIN LASING EXPERIMENTS
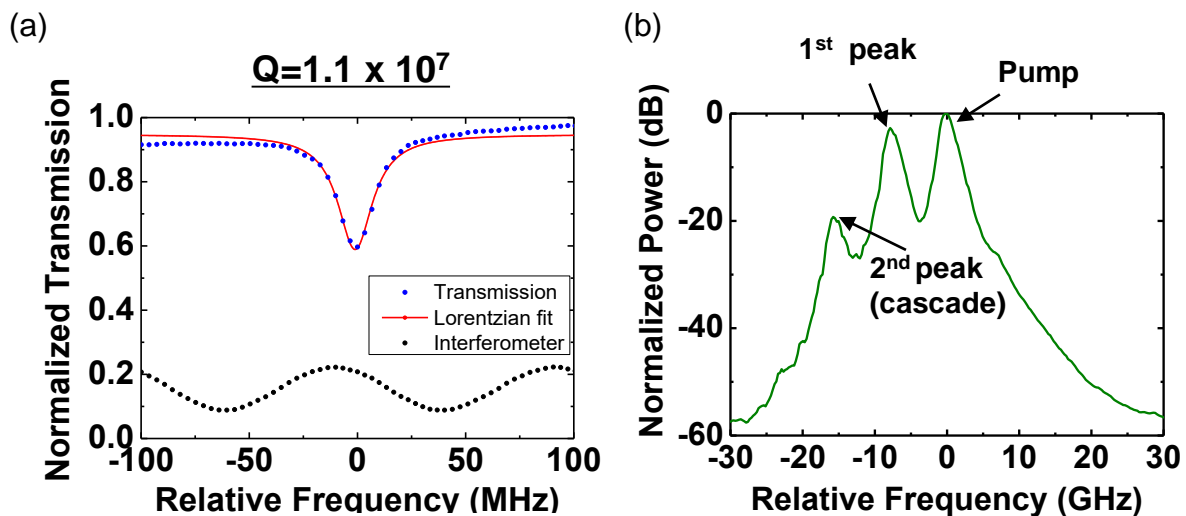

Figure 5. Measured data of the trapezoidal ring cavity. (a) Transmission spectrum of a waveguide coupled with a trapezoidal ring resonator. The quality factor of the resonator can be calculated from full width at half maximum of the Lorentzian fitting, and the value of the quality factor is 1.1×10^7. (b) The measured spectrum of the Brillouin lasing measured with optical spectrum analyzer. Lasing threshold is measured below 1 mW. With higher power we see cascaded lasing peaks.

By finely tuning the wavelength of the laser, we obtained the transmission spectrum of the waveguide coupled to the resonator near resonant wavelength of the resonator. Figure 5(a) shows the measured transmission spectrum of the waveguide coupled to the resonator. By fitting the measured spectrum with Lorentzian function, we obtained the quality factor of the resonator as 1.1×10^7. This Q-factor value is 10 times larger than that of the previous world record of on-chip chalcogenide resonators from other groups [3]. With our new fabrication method, we designed and fabricated ring resonators for stimulated Brillouin lasing experiments [15,16]. The top width, As_2S_3 film thickness, and the angle of the wedge are 10 µm, 1.3 µm, and 30°, respectively. The dimeter of the ring resonator is set to 4.9 mm to match its free spectral range to the Brillouin frequency shift of As_2S_3 material which is around 7.6 GHz. The resonator is pumped through the coupled waveguide with wavelength near 1550 nm. The lasing is observed with pump power less than 1 mW. This value is a dramatic improvement compared to previous record value from other groups which are on the order of few tens of milliwatts [4]. With additional pump power, cascaded lasing has been observed. The spectrum of the Brillouin lasing measured by an optical spectrum analyzer (OSA) is shown in Fig. 5(b).

6. SUMMARY

We have proposed and experimentally demonstrated the new fabrication method for fabricating high-Q chalcogenide devices on a chip which avoids direct etching of chalcogenide films. The surface roughness of the fabricated devices is dramatically reduced (below 1 nm) as confirmed by AFM measurement. The Q-factor of the ring resonator fabricated by the new method is 1.1×10^7 which is ten time larger than the previous record of on-chip chalcogenide resonators from other groups. The flip-chip coupling scheme is introduced to efficiently couple the resonators with the waveguide on a chip. Also, the Brillouin laser has been successfully implemented using the new method. The threshold power of the laser is measured below 1 mW which is a dramatic improvement compared to the previous world record from other groups which are on the order of few tens of milliwatts [4]. We believe that this new device platform opens a promising route to implement high-Q non-linear devices on chips using chalcogenide materials.

REFERENCES

[1]   Eggleton, B. J., Luther-Davies, B. and Richardson, K., "Chalcogenide photonics," Nat. Photonics **5**(3), 141–148 (2011).

[2]   Karim, M. R., Rahman, B. M. A. and Agrawal, G. P., "Mid-infrared supercontinuum generation using dispersion-engineered Ge_115As_24Se_645 chalcogenide channel waveguide," Opt. Express **23**(5), 6903 (2015).

[3]   Madden, S. J., Choi, D.-Y., Bulla, D. A., Rode, A. V., Luther-Davies, B., Ta'eed, V. G., Pelusi, M. D. and Eggleton, B. J., "Long, low loss etched As2S3 chalcogenide waveguides for all-optical signal regeneration," Opt. Express **15**(22), 14414 (2007).

[4]   Kabakova, I. V., Pant, R., Choi, D.-Y., Debbarma, S., Luther-Davies, B., Madden, S. J. and Eggleton, B. J., "Narrow linewidth Brillouin laser based on chalcogenide photonic chip," Opt. Lett. **38**(17), 3208 (2013).

[5]   Kim, W. H., Nguyen, V. Q., Shaw, L. B., Busse, L. E., Florea, C., Gibson, D. J., Gattass, R. R., Bayya, S. S., Kung, F. H., Chin, G. D., Miklos, R. E., Aggarwal, I. D. and Sanghera, J. S., "Recent progress in chalcogenide fiber technology at NRL," J. Non. Cryst. Solids **431**, 8–15 (2016).

[6]   Morrison, B., Casas-Bedoya, A., Ren, G., Vu, K., Liu, Y., Zarifi, A., Nguyen, T. G., Choi, D.-Y., Marpaung, D., Madden, S., Mitchell, A. and Eggleton, B. J., "Compact Brillouin devices through hybrid integration on Silicon," 2017.

[7]   Dianov, E. M., Petrov, M. Y., Plotnichenko, V. G. and Sysoev, V. K., "Estimate of the minimum optical losses in chalcogenide glasses," Sov. J. Quantum Electron. **12**(4), 498–499 (2005).

[8]   Zakery, A. and Elliott, S. R., "Optical properties and applications of chalcogenide glasses: A review," J. Non. Cryst. Solids **330**(1–3), 1–12 (2003).

[9]   Lee, H., Chen, T., Li, J., Yang, K. Y., Jeon, S., Painter, O. and Vahala, K. J., "Chemically etched ultrahigh-Q wedge-resonator on a silicon chip," Nat. Photonics **6**(6), 369–373 (2012).

[10]   Soref, R. A., Schmidtchen, J. and Petermann, K., "Large Single-Mode Rib Waveguides in GeSi-Si and Si-on-SO2," 1971–1974 (1991).

[11]   Pfeiffer, M. H. P., Liu, J., Geiselmann, M. and Kippenberg, T. J., "Coupling Ideality of Integrated Planar High-Q Microresonators," Phys. Rev. Appl. **7**(2), 1–9 (2017).

[12]   Spillane, S. M., Kippenberg, T. J., Painter, O. J. and Vahala, K. J., "Ideality in a fiber-taper-coupled microresonator system for application to cavity quantum electrodynamics.," Phys. Rev. Lett. **91**(4), 043902 (2003).

[13]   Knight, J. C., Cheung, G., Jacques, F. and Birks, T. A., "Phase-matched excitation of whispering-gallery-mode resonances by a fiber taper," Opt. Lett. **22**(15), 1129 (1997).

[14]   Cai, M., Painter, O. and Vahala, K. J., "Observation of Critical Coupling in a Fiber Taper to a Silica-Microsphere Whispering-Gallery Mode System," Phys. Rev. Lett. **85**(1), 74–77 (2000).

[15]   Eggleton, B. J., Poulton, C. G. and Pant, R., "Inducing and harnessing stimulated Brillouin scattering in photonic integrated circuits," Adv. Opt. Photonics **5**, 536–587 (2013).

[16]   Li, J., Lee, H., Chen, T. and Vahala, K. J., "Characterization of a high coherence, Brillouin microcavity laser on silicon," Opt. Express **20**(18), 20170 (2012).